# A Theoretician's View of the C–F Bond Activation Mediated by the Lanthanide Cations $Ce^+$ and $Ho^+$

**Roland H. Hertwig and Wolfram Koch*[a]**

**Abstract:** The mechanistic details of the fluorine transfer reaction $Ln^+ + F-R \rightarrow LnF^+ + R$ with fluoromethane and fluorobenzene as substrates F–R have been elucidated by using quantum chemical techniques. We have chosen two lanthanide monocations, $Ce^+$ and $Ho^+$ as representatives for the early and rather reactive rare earth elements with low second ionization energy (IE) ($Ce^+$) and the late and less reactive elements possessing a higher second IE ($Ho^+$). The reaction path of the defluorination process of the two fluorohydrocarbons $CH_3F$ and $C_6H_5F$ brought about by these cations was mapped by determining all relevant stationary points, that is, reactants, intermediates, saddle points, and products along the reaction coordinate. The occurrence of two competing different reaction paths is the key for a rationalization of the counterintuitive experimental observation of a higher reactivity of fluorobenzene compared to fluoromethane in spite of its significantly larger C–F bond strength.

**Keywords:** cations · density functional calculations · lanthanides · reaction mechanisms

## Introduction

The replacement of hydrogen with fluorine provokes a marked change of physical and chemical properties of hydrocarbons as they are turned into fluorohydrocarbons (FHC) or even saturated fluorocarbons (FC).[1] FHC and FC are chemically robust and possess a high thermal stability. These and other properties make fluorinated organic substrates attractive for a number of applications, such as refrigerants or pesticides. Unfortunately, it is this persistence, together with their large-scale industrial production, that has led to an accumulation of FHC and FC in the environment, which raises the question of their degradation. The enhanced stability of fluorocarbons compared to hydrocarbons is reflected in a remarkably high dissociation energy for C–F bonds (110–130 kcal mol$^{-1}$) as opposed to about 100 kcal mol$^{-1}$ for C–H bonds. Selective metal-mediated activation of carbon–fluorine bonds is still a formidable task, both from an experimental and theoretical perspective. Hence, it has only scarcely been addressed in the literature, in most cases by employing transition metal compounds.[2] Even less is known about the ability of rare earth compounds to activate fluorinated hydrocarbons, in spite of the increasing use of lanthanides in many areas of modern technology, such as heterogeneous catalysis, superconductivity, advanced materials, and their growing impact on organometallic chemistry.[3] In an attempt to unravel the intrinsic properties of the lanthanides in the C–F bond activation processes, mass spectrometric experiments on the gas-phase reactions of all lanthanide monocations $Ln^+$ with fluorobenzene and several other fluorohydrocarbons have been studied by Cornehl, Hornung, and Schwarz.[4] Although C–F bonds are principally stronger than C–C and C–H bonds, the activation of C–F bonds was observed with almost all lanthanide cations for certain fluoroorganic substrates. This was in remarkable contrast to the results of an earlier investigation of the corresponding reactions between $Ln^+$ ions and hydrocarbons.[5] In this study, a mechanism was suggested which involves the oxidative addition of the $Ln^+$ into a C–H or C–C bond, and therefore two reactive, that is, non-4f electrons are required.[6] Indeed, only those $Ln^+$ ions that possess two non-f valence electrons (that is, $La^+$, $Ce^+$, $Gd^+$) or at least involve a low excitation energy to access such a state (that is, $Pr^+$, $Tb^+$) where found to be reactive. The reactivity of lanthanide monocations towards C–F bond activation did not show a similar dependence from the $f^n(sd)^1 f^{n-1}s^1d^1$ excitation energies. Rather, Cornehl, Hornung, and Schwarz[5] were able to correlate the relative reaction rates found in the gas-phase to the second ionization energy (IE) of the respective elements. Thus, the electron transfer from $Ln^+$ towards the fluorine upon formation the $Ln^+$–F bond must be the decisive factor of the reaction and a harpoon type mechanism, that is, a direct abstraction of fluorine by the lanthanide cation was suggested. This scenario of reductive defluorination, schematically

[a] Prof. Dr. W. Koch, Dr. R. H. Hertwig[+]
Institut für Organische Chemie der Technischen Universität Berlin, Strasse des 17. Juni 135, D-10623 Berlin (Germany)
Fax: (+49) 30-314-21102
E-mail: kochw@argon.chem.tu-berlin.de.

[+] Present address: CII Consulting Group GbR, Mohrenstrasse 69, D-10117 Berlin (Germany)



0947-6539/99/0501-0312 $ 17.50+.50/0 *Chem. Eur. J.* **1999**, *5*, No. 1

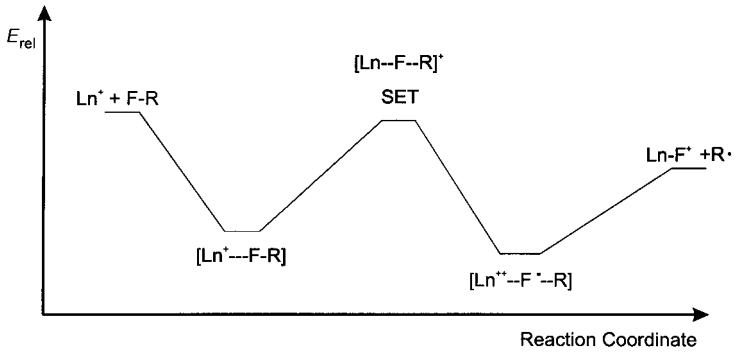


Figure 1. Harpoon-type mechanism suggested for the reductive defluorination.

depicted in Figure 1, involves a single electron transfer (SET) from the lanthanide cation towards fluorine upon formation of the Ln–F bond. A similar mechanism was very recently computationally established for the related reaction between the main group metal ion $Ca^+$ and $CH_3F$.[7]

This model is consistent with the observed high reactivity of the early lanthanide monocations such as $Ce^+$ and $Pr^+$, which are characterized by rather low second ionization energies, and a much lower reactivity of late ones like $Ho^+$ and $Tm^+$, where the second IE is high.[4] It also explains the absence of dehydrohalogenation products (e.g. methylene or unsaturated hydrocarbons) for most lanthanide cations which would be an obvious consequence of an insertion/elimination reaction mechanism. A further consequence of the postulated harpoon-type mechanism is that the electron transfer should not only depend on the IE of the respective lanthanide monocation but also on the bond strength of the C–F bond being broken! However, Cornehl, Hornung, and Schwarz found that $Ln^+$ ions activated the C–F bond of fluorobenzene with *higher* relative reaction rates than those found in the reaction with fluoromethane in spite of the significantly stronger C–F bond energy of $C_6H_5F$ ($125.3 \pm 2.3$ kcal mol$^{-1}$)[8] compared to $CH_3F$ ($112.0 \pm 0.3$ kcal mol$^{-1}$)![8] While it was speculated that short lifetimes of the ro-vibrationally excited encounter complexes and/or other kinetic barriers along the reaction path could be responsible for this unexpected lower efficiency of $CH_3F$ as compared to $C_6H_5F$,[5] no clear-cut interpretation could be given at that time. It is the aim of the present contribution to use quantum chemical techniques to shed some light on the details of the $Ln^+$-mediated C–F bond activation in these two substrates and to provide an answer to this mechanistic puzzle. We have chosen two lanthanide monocations, $Ce^+$ and $Ho^+$ as representatives for the early and rather reactive rare earth elements with low second IE ($Ce^+$) and the late and less reactive elements possessing a higher second IE ($Ho^+$). The reaction path of the defluorination process of the two fluorohydrocarbons $CH_3F$ and $C_6H_5F$ brought about by these cations was mapped by determining all relevant stationary points, that is, reactants, intermediates, saddle points, and products along the reaction coordinate. Due to the convincing experimental evidence that a insertion/elimination mechanism can be ruled out,[4] only the direct fluorine abstraction mechanism was considered.

## Theoretical Approach and Computational Details

Theoretical studies on lanthanide complexes are relatively rare in the literature[9] and density functional theory (DFT) based methods which have been established as useful in the theoretical treatment of d transition metal elements[10] have only seldom been applied to rare earth element containing molecules.[11] Most theoretical studies are concerned with inorganic compounds, for example neutral Ln–dimers,[12] Ln–monohalides and Ln–monoxides.[13] A combined theoretical and experimental study that investigated cationic cerium dioxide[14] states that DFT methods are in good agreement with various correlated ab initio methods. Apart from the considerations that apply in general for open-shell transition metal complexes,[9] lanthanide-containing compounds pose high demands in terms of computing resources, since f-type basis functions are necessary because of the occupied 4f orbitals. Polarized basis sets must therefore go even beyond this level, that is basis functions of $l$ quantum number $\geq 4$ ($g$ functions) are required. The use of relativistically adjusted effective core potentials (RECP) on the metal is mandatory to account for the (kinematical) relativistic effects. The strategy adopted in the present study relies on the B3LYP functional[15] as an accurate but at the same time economical method for the determination of structures and relative energies. Three different RECP/basis set combinations have been employed. In a first set of calculations an RECP/basis set by Cundari and Stevens[16] that employ a [Kr 4d$^{10}$] core and a (6s,6p,3d,7f)/[4s,4p,2d,3f] contraction for the valence space was used for the metal. For the main group elements the standard D95 double-$\zeta$ basis set[17] was employed. This combination, which is termed BSI, was only used for geometry optimizations and frequency determinations. BSII consists of the 28MWB RECP/basis set by Dolg et al.[18] which translates into the smaller [Ar 3d$^{10}$] core (that is, only 28 electrons are covered by the RECP) and a (12s,11p,9d,8f)/[9s,8p,6d,5f] contraction to be used for the lanthanide, and the standard 6-31G** basis sets on carbon and hydrogen. For fluorine this basis set was augmented by one diffuse s- and p-function, that is, the 6-31+G** contraction.[19] For the resulting structures of the $[Ln,F,C,H_3]^+$ system, relative energies were re-calculated with the single-reference based averaged coupled pair functional[20] (ACPF) in order to check the reliability of the density functional approach. For these energy determinations a larger basis set (BSIII) was constructed by augmenting the 28MWB RECP/basis set combination with two $g$-polarization functions ($\alpha = 2.5$ and 6.0) to recover angular correlation effects on the metal, while a DZP basis set was used for all other elements, augmented by one diffuse p-function on fluorine.[18] On the metal, the 5s, 5p, 4f, 5d and 6s electrons were correlated, while for F and C all but the 1s electrons were included in the correlation treatment. For the larger $[Ln,F,C_6,H_5]$ system, the ACPF calculations turned out to be extremely time consuming and are therefore restricted to few selected examples. The force constant matrices were obtained at the B3LYP/BSI level of theory by numerical differentiation of the analytical gradients to characterize all stationary points found on the $[Ln,F,C,H_3]^+$ potential energy surface (PES) as minima or saddle points. The harmonic frequencies were also used to correct the total energies for zero-point vibrational energies (ZPVE) and to convert the energies to Gibbs free energies at 298 K which guarantees a maximum of compatibility with experimental data. For the $[Ln,F,C_6,H_5]^+$ species, calculation of the force constant matrices turned out to be prohibitively resource intensive. The determination of vibrational frequencies for the stationary points on this PES however, does not primarily serve to identify the character of the stationary points as minima or saddle points since they should be analogous to those of the $Ln^+$/fluoromethane system. Nevertheless, without harmonic frequencies no thermal corrections can be determined. The approach we adopted to solve this problem is very pragmatic but efficient. The harmonic vibrational frequencies were calculated only for the encounter complex (Min(1)) and a transition structure (TS(1)) on the $[Ce,F,C_6,H_5]^+$ PES. To a first approximation, these were then assumed to be constant for similar types of molecular arrangements and those determined for Min(1) were used for other minima, whereas the frequencies determined for TS(1) were also used for other transition structures. The justification for this admittedly very crude procedure is the observation that in the $Ln^+/CH_3F$ system similar types of molecules possess very similar ZPVE and thermal corrections (within 2 kcal mol$^{-1}$). For the $[Ho,F,C_6,H_5]^+$ PES we went even one step further and used the force constants of the analogous stationary points on the $[Ce,F,C_6,H_5]^+$ PES. The corresponding frequencies were calculated by

  0947-6539/99/0501-0313 $ 17.50+.50/0 

simply setting the mass of the metal to that of Ho. Again, tests of this procedure performed for the $[Ln,F,C,H_3]^+$ PES (where the force constants for all compounds were calculated explicitly) yielded reasonable agreement with the actual thermodynamic corrections, since also the structural features of the cerium and holmium complexes are similar. The uncertainty introduced by this method is estimated to be within $\pm 3$ kcal mol$^{-1}$. Thus, although from a purist point of view this procedure is all but immaculate, it furnishes useful results in the present case. A further source of error is introduced by the complete neglect of spin–orbit interactions in our calculations. Since these interactions will be stronger in the free atom than in molecules, the relative energies of the entrance channels $Ln^+ + F-R$ will probably be somewhat overestimated. Overall, we expect that the computational strategy furnishes results with error bars of the order of at least $\pm 5$ kcal mol$^{-1}$. The wave functions[21] obtained at the B3LYP/BSII level were analyzed with the natural bond orbital (NBO) method.[22]

The following programs were used: MULLIKEN[23] (geometry optimizations and harmonic frequencies), MOLPRO96[24] (ACPF calculations) and GAUSSIAN94[25] (NBO analysis).

## Results and Discussion

**Calibration**: The first step in a computational endeavor such as this must consist in a careful calibration of the chosen computational strategy so that the level of confidence that can be expected from the theoretical strategy can be assessed. Unfortunately, a direct comparison between theoretically predicted and experimental data is difficult, because only little is known of complexes between bare lanthanide cations and organic molecules. Since the second IE of the metal is among the decisive factors determining the reactivity of a rare earth cations towards C–F bond activation, the capability to reproduce this property is a first indication for the predictive power of the computational techniques. The data in Table 1 show that both levels of theory, B3LYP/BSII and ACPF/BSIII give second IE in good agreement with experiment (maximum deviation of 0.2 eV for Ce). Further, the thermodynamic features of the defluorination reaction are dependent on an adequate description of the $Ln^+$–F bonds which are formed in the process. Since an experimental estimate exists only for $HoF^+$, for $CeF^+$ the internal consistency of the theoretical methods used has to suffice to estimate their adequacy. The standard bond enthalpies of the cationic cerium and holmium fluorides are included in Table 2. Interestingly, the B3LYP/BSII values do not exhibit the DFT-typical overbinding in comparison to the ACPF data; in fact they are 5–8 kcal mol$^{-1}$ lower. For $CeF^+$, no experimental binding energy exists but since the variations among the B3LYP and ACPF data are comparable to those found for $Ho^+$, it can be concluded that both, the B3LYP/BSII and the ACPF/BSIII approaches are in good agreement with the sparse experimental data. The theoretically predicted data suggest that the hitherto unknown $CeF^+$ bond dissociation energy should lie around 150 kcal mol$^{-1}$. As an aside, we note that the difference in the Ln–F binding energies between cerium and holmium turns out to be almost identical to the differences between their second IEs (ca. 1 eV or 23 kcal mol$^{-1}$). Finally, the accuracy of calculations on the defluorination reaction also relies on the accurate reproduction of the C–F bond strengths. A comparison of the experimental and theoretical C–F binding energies for fluoromethane and fluorobenzene is given in Table 3. The B3LYP/BSII results are in excellent agreement with experiment, even better than the ACPF values. Thus, the calibration calculations point to a reliability of the two computational approaches sufficient for obtaining semiquantitatively correct results even for systems as complex as the present ones.

Table 1. Experimental and calculated second ionization energies for Ce and Ho [eV].

| $Ln^+$ | UB3LYP/BSII | ACPF/BSIII | Exp.[a] |
|---|---|---|---|
| Ce | 10.6 | 11.1 | 10.8 |
| Ho | 11.9 | 11.6 | 11.8 |

[a] Ref. [29].

Table 2. Experimental and calculated bond enthalpies for $CeF^+$ and $HoF^+$ [kcal mol$^{-1}$].

| $LnF^+$[a] | UB3LYP/BSII | ACPF/BSIII | Exp. |
|---|---|---|---|
| $CeF^+$ $^3\Sigma$ ($f_\phi^1 f_\phi^1$) | 144.6 | 152.2 | – |
| $HoF^+$ $^4$ ($f_\phi^1 f_\phi^1 f_\pi^1$) | 123.3 | 128.8 | $127 \pm 7$ [b] |

[a] R[Ce–F] = 2.066 Å, R[Ho–F] = 1.986 Å (B3LYP/BSII). [b] Ref. [5].

Table 3. Experimental and calculated C–F bond enthalpies [kcal mol$^{-1}$].

| R–F | B3LYP/BSII | ACPF/BSIII [a] | Exp |
|---|---|---|---|
| $CH_3$–F | 106.5 | 103.0 | 107.7 |
| $C_6H_5$-F | 124.0 | 119.9 | 125.3 |

[a] At B3LYP/BSII geometries.

**The $[Ln,F,C,H_3]^+$ system**: Figure 2 displays the structures of the relevant stationary points along the reaction coordinate of the reaction between bare $Ce^+$ or $Ho^+$ and fluoromethane computed at B3LYP/BSII (it should be noted that very similar geometries result from using BSI). Table 4 lists the corresponding energetic information obtained with the B3LYP/BSII and ACPF/BSIII methods.

In the following, the discussion of the mechanistic features will be carried out simultaneously for $Ce^+$ and $Ho^+$, thereby identifying differences and elements in common for both cases. Since the mechanistic element of bond insertion can be ruled out (see above), the number of bonds formed throughout the process equals the number of bonds that are cleaved. Taking into account that these bond-breaking/bond-formation processes occur in a homolytic manner, the overall number of singly occupied orbitals is not expected to vary and the sum of unpaired electrons encountered in the entrance channel is preserved throughout the reaction ($S = 3/2$ for $Ce^+$, $S = 2$ for $Ho^+$ and $S = 0$ for $CH_3F$). Therefore, we restricted ourselves to the quartet ($S = 3/2$) and the quintet ($S = 2$) hypersurfaces for the $Ce^+$ and $Ho^+$ fluoromethane systems, respectively.

Starting from the separated reactants, the first minimum, Min(1), is a mostly electrostatically bound encounter complex between the ground state $Ce^+$ ($^4H$) or $Ho^+$ ($^5I$) ions, respectively, and fluoromethane (NBO charges on $Ce^+$ and $Ho^+$ are 0.98 and 1.00, respectively, and spin density located exclusively on the metal). Interestingly, the bond strength



0947-6539/99/0501-0314 $ 17.50+.50/0 *Chem. Eur. J.* **1999**, *5*, No. 1

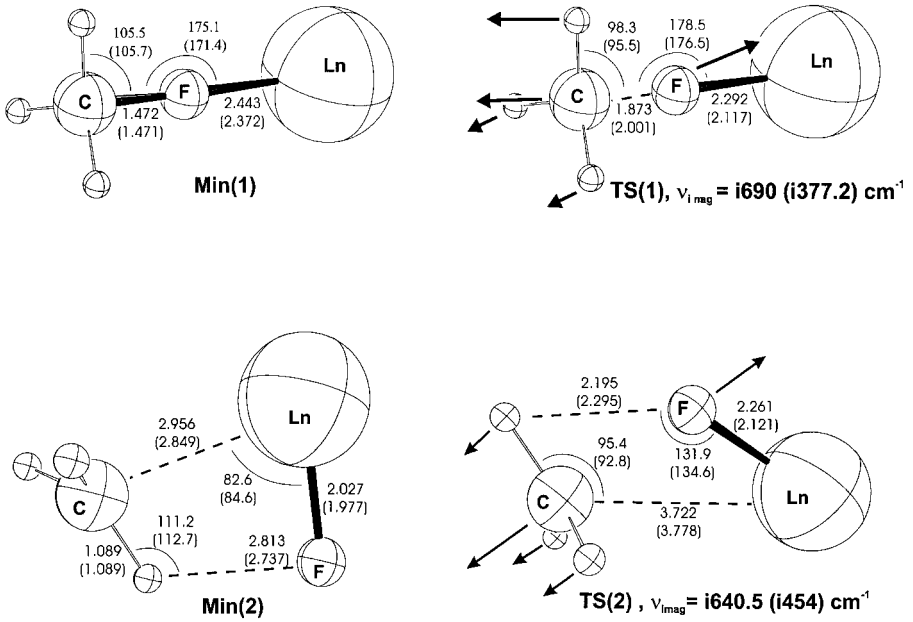


Figure 2. Relevant stationary points on the [Ln,C,$H_3$,F] PES. Bond lengths in Å, angles in degrees, computed at B3LYP/BSII. For the saddle points, the major components of the transition modes are also shown.

Table 4. Relative Gibbs free energies of stationary points on the $[Ln,F,C,H_3]^+$ PES [kcal mol$^{-1}$].

| Structure | B3LYP/BSII | ACPF/BSIII[a] | B3LYP/BSII | ACPF/BSIII[a] |
|---|---|---|---|---|
| | Ln = Ce | | Ln = Ho | |
| $Ln^+$ $CH_3F$ | 0.0 | 0.0 | 0.0 | 0.0 |
| Min(1) | –27.0 | –26.0 | –14.6 | –12.9 |
| TS(1) | –9.0 | –14.5 | –2.5 | –[b] |
| TS(2) | –7.9 | –18.4 | –0.8 | –[b] |
| Min(2) | –57.9 | –57.2 | –32.2 | –[b] |
| $LnF^+ + {}^{\cdot}CH_3$ | –40.7 | –51.9 | –19.4 | –30.0 |

[a] At B3LYP/BSII geometries. [b] No ACPF data due to technical problems, see text.

between fluoromethane and $Ce^+$ turns out to be almost twice as high (27 or 26 kcal mol$^{-1}$ at B3LYP/BSII and ACPF/BSIII, respectively) than that of $Ho^+$ (15 and 13 kcal mol$^{-1}$). Thus, it seems as if the more pronounced fluorophilicity of $Ce^+$ compared to $Ho^+$ as observed for the cationic fluorides (see above) is visible already in these complexes. The C–F bonds are some 0.07 Å longer than those in isolated $CH_3F$ (1.399 Å with BSII) which hints to some additional covalent interaction. The natural electron configurations of cerium and holmium are $6s^{0.90}4f^{1.77}5d^{0.40}$ and $6s^{0.96}4f^{11.07}5d^{0.03}6p^{0.02}$, respectively, in the Ln–$FCH_3$ complex. For cerium, this strongly deviates from the ground state of the cation ($Ce^+$: $4f^15d^2$) and is related to that of the dication ($Ce^{++}$: $4f^2$), whereas for holmium ($Ho^+$: $6s^14f^{11}$) only marginal deviations from the atomic occupations of the cation are observed. While the change of the population on $Ce^+$ certainly costs excitation energy, this is obviously counterbalanced by an optimized bonding as the $Ce^+/FCH_3$ complex benefits from 1.30 electrons in non-f orbitals. As the natural hybridization analysis of the HOMO indicates ($sd^{0.15}$ character) a partial hybridization of the 6s and 5d orbitals takes place to optimize the covalent terms in the bonding to the fluorine. On the other hand, $Ho^+$ has a singly occupied 6s orbital. The energetical costs to obtain configurations with more than one non-f orbital are higher than for $Ce^+$, since one of the low-lying f electrons must be excited. Thus, formation of sd hybrids is less likely in $Ho^+/FCH_3$. Indeed, the natural hybridization analysis shows an only weak d contribution to the HOMO ($sd^{0.02}$). The existence of a side-on minimum was checked carefully but all attempts ended up in the quasi-linear structures.

The exclusive existence of an almost $C_{3v}$-symmetric encounter complex supports the notion of a direct abstraction reaction mechanism with a de facto linear Ln-F-C arrangement throughout the entire reaction sequence. Thus, one would expect that also the transition structure should not deviate from the linear arrangement. In fact, an almost linear transition state (TS) was located. The relative energies for this TS(1) are determined as –9.0 (B3LYP/BSII) and –14.5 kcal mol$^{-1}$ (ACPF/BSIII) for $Ce^+$. If the reaction is carried out with $Ho^+$ the height of this barrier lies much closer to the entrance channel (–2.5 kcal mol$^{-1}$). In this case no ACPF calculation could be performed due to insurmountable technical problems, due to an increasing multideterminatal character of the wave function. Relative to Min(1), the C–F bond is elongated significantly to 1.873 Å in TS(1) on the $[Ce,F,C,H_3]^+$ PES or even to 2.001 Å for the analogous holmium containing structure. This is accompanied by a shortened $Ln^+$–F bond of 2.292 Å and 2.117 Å for $Ce^+$ and $Ho^+$, respectively. The imminent C–F bond cleavage results in a flattening of the $CH_3$ unit (deviation from planarity amounts to only 6–9°) which correlates with a significant radical character on the carbon atom. In the NBO analysis a spin density of 0.28 units is assigned to the carbon atom with a concomitant reduction to 2.70 on cerium. Fluorine maintains a value of 0.02. Similar data are obtained for the holmium case with 0.22 on carbon, 0.02 on fluorine, 3.54 on the metal. In accordance with the SET shown in Figure 1 the partial charge on the metal has increased from 1.00 to 1.22 for cerium and to 1.39 for holmium. As expected, the bonding situation of TS(1) is intermediate to Min(1) and the products of the defluorination reaction, that is, a methyl radical and $LnF^+$. In spite of a careful search, no electrostatic complex between a $LnF^+$ ion and a $CH_3$ radical, preceding the separated products, could be located. However, what we did find was Min (2), a four-membered ring complex with interactions between the carbon atom of the methyl radical and the positively charged $Ln^+$ ion as well as between the negatively polarized fluorine of the $LnF^+$ moiety and one of the hydrogen atoms of the methyl radical. Actually, Min(2) represents the lowest lying point on

this reaction coordinate, being some 58 kcal mol$^{-1}$ below the entrance channel for Ce (B3LYP/BSII and ACPF/BSIII) and 32 kcal mol$^{-1}$ below the $Ho^+ + CH_3F$ asymptote at B3LYP/BSII. Again, for technical reasons, no ACPF results could be obtained for Min(2). The existence of Min(2) suggests a transition structure connecting Min(1) and Min(2) with a bent Ln-F-C arrangement. Indeed a second saddle point with the expected geometry was located (TS(2)). For Ce, the relative energy of TS(2) amounts to $-7.9$ and $-18.4$ kcal mol$^{-1}$ at B3LYP/BSII and ACPF/BSIII, respectively. For Ho, we again can only give a B3LYP/BSII barrier height, which amounts to $-0.8$ kcal mol$^{-1}$. Nevertheless, for both metals the two transition structures, TS(1) and TS(2) are similar in energy and it must be concluded that there do exist two discrete pathways leading from the reactants $CH_3F + Ln^+$ to the products $CH_3 + LnF^+$, but that they are energetically almost identical. Finally, the relative energy of the exit channel lies well below that of the entrance channel for both metals, $-40.7$ (B3LYP/BSII) and $-51.9$ (ACPF/BSIII) for Ce and $-19.4$ (B3LYP/BSII) and $-30.0$ (ACPF/BSIII) for Ho, respectively. This high overall exothermicity is of course due to the remarkable $Ln^+-F$ bond strengths.

In Figure 3, we show the B3LYP/BSII based natural atomic charges which indicate a continuous transfer of one electron from the lanthanide cation towards the fluorine in the course of the defluorination reaction in line with the conception of the harpoon-type mechanism. At the saddle points of the reaction, about one third of an electron has migrated towards the fluorine as indicated by the decrease of the partial charge on the metal by around 0.3–0.4 $|e|$ at the locations of the transition structures TS(1) and TS(2). Concomitantly, the spin density on the carbon atom builds up by a similar amount. This synchronous transfer of charge and spin density can be seen across the whole reaction coordinate. Thus, the leading motif in the reaction seems to be the preservation of a formal closed-shell character at fluorine (i.e., as a $F^-$ ion), where hardly any spin density is found.

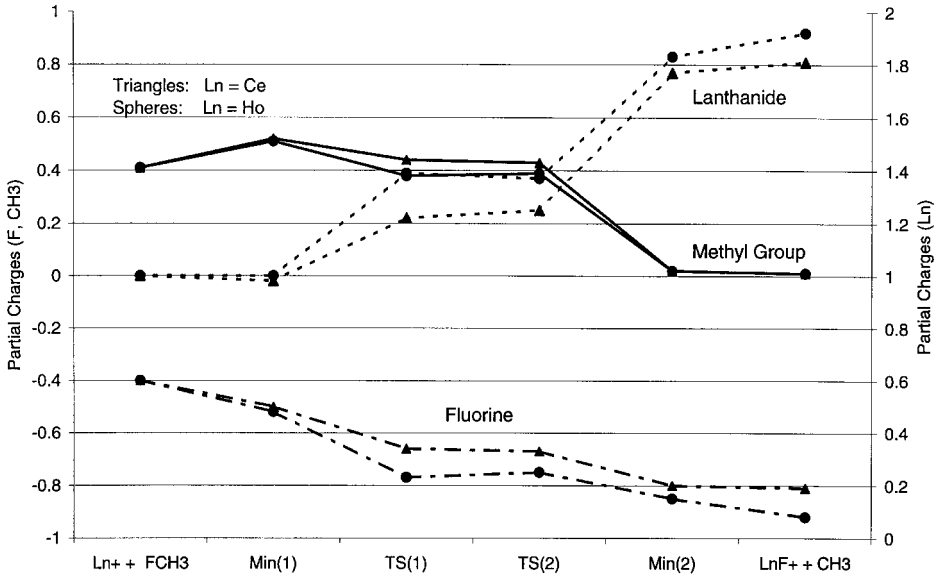


Figure 3. Partial charges (NBO at B3LYP/BSII) along the reaction coordinate.

There is still one question which has not been addressed yet: W*hy* are there two distinct saddle points, one with an almost linear and the other with an L-shaped Ln-F-C arrangement, which correspond to two different reaction paths for the overall fluorine transfer reaction? At first glance this result is confusing, since for the encounter complex Min(1) the potential for bending the Ln-F-C angle was found to be repulsive, with the linear coordination as the only minimum. The key for understanding this effect is that although in the end, it acts as charge donor, the metal cation is primarily attracted by the nucleophilic character of the partially negatively charged fluorine. Hence, the trajectory in which the two reactants approach should be the one which allows a maximization of attractive electrostatic interaction. It was shown by Bader[26] through his atoms-in-molecules approach that, apart from the direction of the $F-CH_3$ dipole, fluoromethane actually shows two more trajectories for an electropilic attack in the H-C-F plane of fluoromethane. One is in a *syn* and the other in the *anti* position to the in-plane hydrogen atom. Thus, in addition to following the $F-CH_3$ dipole, an electrophile should indeed also approach fluoromethane in a perpendicular manner, specifically in *anti* position to the in-plane hydrogen atom to minimize steric effects, leading to TS(1) and TS(2), respectively.

To summarize, both metals exhibit identical reaction paths in a harpoon-type abstraction mechanism. Two approximately energetically degenerate transition structures have been identified, one with a *quasi* linear Ln-F-C arrangement, whereas the other displays a bent Ln-F-C structural element. In qualitative agreement with the experimental relative reactivities, the activation barriers are smaller for $Ce^+$ than for $Ho^+$. The driving force of the reaction is the formation of a strong $Ln^+-F$ bond. Both, $CeF^+$ and $HoF^+$ are almost completely ionic in nature and their bond strengths are directly related to the second IE of the metal.

**The $[Ln,F,C_6,H_5]^+$ System**: Table 5 contains the theoretically predicted Gibbs free energies (B3LYP/BSII), while Figure 4 shows the optimized geometries (B3LYP/BSI) of the stationary points.

In contrast to $CH_3F$, aromatic ligands may also offer their $\pi$ system as a coordination site. Therefore, three possibilities for a coordination of an $Ln^+$ ion to fluorobenzene to generate the encounter complex were investigated. 1) End-on coordination of the metal cation fluorine, as found to be the case for fluoromethane. 2) Side-on coordination to the C–F bond. Just as for $CH_3F$, also in the present case, this coordination was not found to represent a minimum on the PES for neither $Ce^+$ nor $Ho^+$. 3) Coordination of the metal cation to

  0947-6539/99/0501-0316 $ 17.50+.50/0 *Chem. Eur. J.* **1999**, *5*, No. 1

Table 5. Relative Gibbs free energies of stationary points on the $[Ln,F,C_6,H_5]^+$ PES [kcal mol$^{-1}$].

| Structure[a] | B3LYP/BSII | ACPF/BSIII | B3LYP/BSII |
|---|---|---|---|
| | Ln = Ce | | Ln = Ho |
| $Ln^+ + C_6H_5F$ | 0.0 | 0.0 | 0.0 |
| Min(3) | – 30.5 | – | – 15.8 |
| Min(4) | – 21.3 | – 23.7 | –[b] |
| TS(3) | – 6.3 | – 5.0 | 20.5 |
| TS(4) | – 10.3 | – | – 3.4 |
| $LnF^+ + C_6H_5$ | – 24.2 | – 36.4 | – 3.2 |

[a] Optimized at B3LYP/BSI. [b] No self consistence could be achieved.

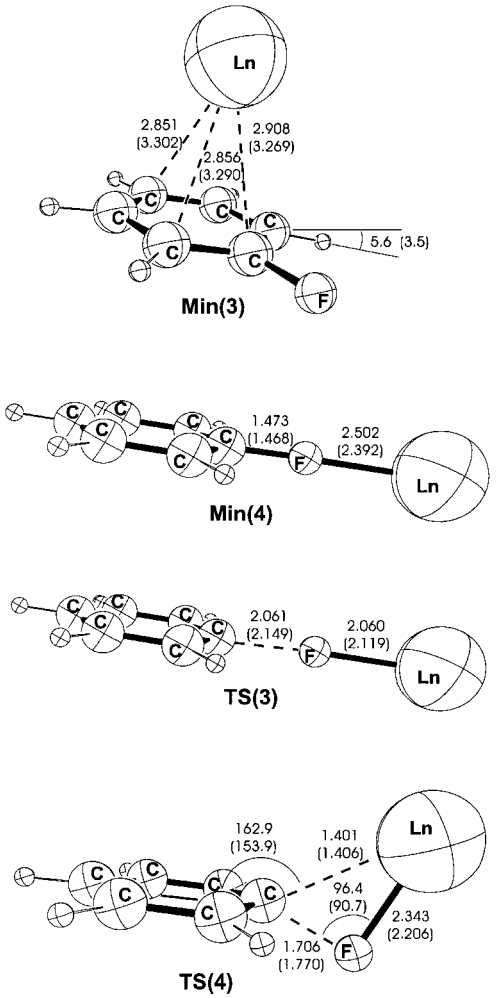


Figure 4. Relevant stationary points on the $[Ln,C_6,H_5,F]$ PES. Bond lengths in Å, angles in degrees, computed at B3LYP/BSI.

the benzenoid π system. As expected, a minimum with the metal cation centered above the aromatic ring could be located, (Min(3)).[27] The B3LYP/BSII energies assign a stronger $Ln^+$–ligand bond to the cerium complex (– 30.5 kcal mol$^{-1}$) than for the corresponding $Ho^+$ complex (– 15.8 kcal mol$^{-1}$). The second encounter complex located on the $[Ln,F,C_6H_5]^+$ PES, Min(4) contains a linear Ln-F-C arrangement and is akin to Min(1). Since the tendency for distortion from linearity was found to be insignificant for the $Ln^+/FCH_3$ system, the computational advantages of the higher symmetry ($C_{2v}$ instead of $C_s$) were used by freezing the Ln-F-C angle at 180°. For $Ce^+/FC_6H_5$ Min(4) is some 9 kcal mol$^{-1}$ less stable than the π complex, Min(3), and is located 21.3 kcal mol$^{-1}$ below the reactants. At the ACPF/BSIII level a similar result, that is, – 23.7 kcal mol$^{-1}$ is obtained. A minimum corresponding to Min(4) was also located for holmium at the B3LYP/BSI level, however, it was impossible to achieve a self consistent Kohn–Sham solution in the B3LYP/BSII single point calculation. Hence, no comparison of the relative energies is possible. The metal–ligand bond in the linear $Ce^+/FC_6H_5$ complex Min(4) is weaker than in the corresponding $Ce^+/FCH_3$ encounter complex Min(1) due to the stronger C–F bond in fluorobenzene. Similarly, the C–F and Ln–F bonds of fluorobenzene are shorter and longer, respectively, than the corresponding contacts in Min(1). Transition structure TS(3) represents the transition state on the $[Ln,F,C_6H_5]$ PES analogous to TS(1). However, its structural features prove TS(3) to be more product-like than TS(1): The C–F distances are longer, while the Ln–F distances are shorter. Also the relative energetics of TS(3) mirror the differences in C–F bond strengths, as expected the activation barrier is higher than in the $CH_3F$ case. While for Ce the relative energy of TS(3) is still below that of the entrance channel (– 6.3 and – 5.0 kcal mol$^{-1}$ at B3LYP/BSII and ACPF/BSIII, respectively), TS(3) is significantly above the energy of the reactants if $Ho^+$ is employed (20.5 kcal mol$^{-1}$ at B3LYP/BSII).[28] All these observations are in full harmony with the stronger C–F bond in $C_6H_5F$ compared to $CH_3F$.

However, these results which are also the intuitively expected ones, contradict the experimental data, which assign a *higher* relative reactivity to fluorobenzene than to fluoromethane. Thus, it seems questionable whether the actual reaction really proceeds along this reaction coordinate. The solution to this puzzle can be found in TS(4). This saddle point is analogous to the side-on TS(2) located on the $[Ln,F,C,H_3]$ PES. However, while in the $Ln^+/FCH_3$ system the two saddle points were almost isoenergetic, the relative energies of TS(4) at the B3LYP/BSII level turn out to be *lower* than that of TS(3) by 4.0 kcal mol$^{-1}$ for $Ce^+$, or even by a significant 23.9 kcal mol$^{-1}$ for $Ho^+$. At the B3LYP/BSII level TS(4) bears an energy of – 10.3 kcal mol$^{-1}$ relative to the entrance channel for $Ce^+$. The barrier is lower than both, TS(1) (– 9.0 kcal mol$^{-1}$) or TS(2) (– 7.9 kcal mol$^{-1}$) on the $[Ce,F,C,H_3]^+$ PES, in concert with the higher reactivity of fluorobenzene towards fluorine abstraction. This is even more pronounced if the reaction is carried out with $Ho^+$. TS(4) lies at – 3.4 kcal mol$^{-1}$ which is not only in much better agreement with the experimental relative reactivity for this system but also plausible in relation to the $Ln^+/FCH_3$ system. The barriers of TS(1) (– 2.5 kcal mol$^{-1}$) and TS(2) (– 0.8 kcal mol$^{-1}$) on the $[Ho,F,C,H_3]^+$ PES are in agreement with a very low reactivity. Consistent with a higher, but still moderate relative reactivity for the same reaction on the $[Ho,F,C_6,H_5]^+$ PES found by Cornehl, Hornung, and Schwarz[5] is the calculated relative energy of TS(4) with Ln = Ho. Thus, for the $CH_3F$ system both reaction pathways are possible, but in the case of fluorobenzene the nonlinear approach via TS(4) is clearly favored. While this change in mechanism can explain the counterintuitive higher reactivity

of fluorobenzene in the gas phase experiments, we still owe an answer to the question *why* the nonlinear arrangement is favored with fluorobenzene as substrate. Perusal of the structural parameters in part explains this result. Quite evidently, TS(4) occurs earlier on the reaction pathway, as the C–F bonds are 0.3–0.4 Å shorter and the Ln–F bonds are longer than those of TS(3). There are two main factors which stabilize TS(4) as compared to TS(2). First, the repulsive and therefore *destabilizing* steric interactions between the lanthanide cation and the two out-of-plane hydrogen atoms exist only for $CH_3F$. Second, the *stabilization* of TS(4) by interaction between the aromatic π-system and the lanthanide cation is not available to TS(2).

In view of the computational effort and the insignificance for the further course of the reaction, we did not attempt to locate complex(es) succeeding TS(4). Finally, the exit channels occur at higher energies for the $Ln^+/FC_6H_5$ system than for the $Ln^+/FCH_3$ counterpart; a direct consequence of the stronger C–F bond in the former. For $[Ho,F,C_6,H_5]^+$ this results in relative energies close to the entrance channel, $-3.2\ kcal\,mol^{-1}$ while $CeF^+C_6H_5$ is $-24.2\ kcal\,mol^{-1}$ lower than the reactants, $Ce^+ + C_6H_5F$ at B3LYP/BSII. It should be noted that the ACPF/BSIII value for the relative stability of $Ce^+ + C_6H_5$ is significantly larger, amounting to $-36.4$ kcal $mol^{-1}$, an obvious consequence of the larger $Ce-F^+$ bond strength obtained at ACPF/BSIII as compared to B3LYP/BSII, see above.

## Conclusions

By the aid of quantum chemical calculations we identified the mechanistic details of the $Ln^+$-mediated C–F bond activation. This enabled the rationalization of the at first glance puzzling experimental result that the reaction $Ln^+ + F-R \rightarrow LnF^+ + R$ occurs with higher rates for $R = C_6H_5$ than for $R = CH_3$ despite the significantly higher C–F bond strength in the former:

1) In agreement with previous assumptions, the mechanism of $Ln^+$ mediated fluorine abstraction is a direct, harpoon-type mechanism. This is in sharp contrast to the insertion/elimination mechanism established for the activation of C–C and C–H bonds.
2) This mechanism is, however, not necessarily confined to a linear attack of the lanthanide cation at the C–F bond. Two reaction channels involving different transition structures were identified. While one maintains a quasi-linear structure, the other displays a bent Ln-F-C arrangement.
3) In terms of the calculated barrier heights, both reaction paths are almost degenerate for the defluorination reaction of fluoromethane. In distinct contrast to that, the linear saddle point is energetically disfavored compared to the angular arrangement for the same reaction with fluorobenzene. Thus, the latter is the preferred route for the reaction between $Ln^+ + C_6H_5F$ to yield $LnF^+ + C_6H_5$.
4) The occurrence of these two scenarios explain the counter-intuitive reactivity pattern of $CH_3F$ and $C_6H_5F$. The reasons for the energetic preference of the nonlinear approach for fluorobenzene lie primarily in the additional stabilization of the saddle point by the aromatic system, which is obviously not possible for $CH_3F$ as substrate.
5) $Ho^+$ is characterized by a weaker fluorophilicity than $Ce^+$, which is directly related to its higher second ionization energy. As a consequence, the barrier of the fluorine abstraction is higher if $Ho^+$ is used as reactant, in harmony with the lower reactivity found in gas-phase experiments.

## Acknowledgments

We thank Prof. H. Schwarz for fruitful discussions and pointing out this problem to us. Helpful discussions with Drs. H. H. Cornehl, C. Heinemann, J. N. Harvey, and G. Hornung are gratefully acknowledged. H. Grauel is thanked for excellent technical support. A generous amount of computer time was provided by the Konrad-Zuse Zentrum für Informationstechnik Berlin. Finally, we are grateful to the Deutsche Forschungsgemeinschaft and the Fonds der Chemischen Industrie for financial support of this work.

[1] For an overview of the many facets of fluorine chemistry see: *Fluorine-Containing Molecules* (Eds.: J. F. Liebman, A. Greenberg, W. R. Dolbier, Jr.), VCH, Weinheim, **1988.**

[2] G. C. Saunders, *Angew. Chem.* **1996**, *108*, 2783; *Angew. Chem. Int. Ed. Engl.* **1996**, *35*, 2615, and references therein.

[3] See, for example, *Handbook on the Physics and Chemistry of the Rare Earths* (Eds.: K. A. Gschneider Jr., L. Eyring), Elsevier, Amsterdam, **1978** and proceeding volumes; *Industrial Applications of the Rare Earth Elements*, (Ed.: K. A. Gschneider, Jr.), American Chemical Society, Washington, DC, **1981**; H. Schumann, J. A. Messe-Marktscheffel, L. Esser, *Chem. Rev.* **1995**, *95*, 865.

[4] H. H. Cornehl, G. Hornung, H. Schwarz, *J. Am. Chem. Soc.* **1996**, *118*, 9960.

[5] H. H. Cornehl, C. Heinemann, H. Schwarz, *Organometallics* **1995**, *14*, 992.

[6] This resembles the mechanistic scenario established earlier for transition metal mediated C–H and C–C activation processes, see, for example, a) M. C. Holthausen, A. Fiedler, H. Schwarz, W. Koch, *Angew. Chem.* **1995**, *107*, 2430; *Angew. Chem. Int. Ed. Engl.* **1995**, *34*, 2282; b) M. C. Holthausen, A. Fiedler, H. Schwarz, W. Koch, *J. Phys. Chem.* **1996**, *100*, 6236; c) M. C. Holthausen, W. Koch, *J. Am. Chem. Soc.* **1996**, *118*, 9932; d) M. C. Holthausen, W. Koch, *Helv. Chim. Acta* **1996**, *79*, 1939.

[7] J. N. Harvey, D. Schröder, W. Koch, D. Danovich, S. Shaik, H. Schwarz, *Chem. Phys. Lett.* **1997**, *278*, 391.

[8] S. G. Lias, J. E. Bartmess, J. F. Liebman, J. L. Holmes, R. D. Levin, W. G. Mallard, *J. Phys. Chem. Ref. Data* **1988**, *17*, Suppl. 1; S. G. Lias, J. F. Liebmann, R. D. Levin, S. A. Kafafi, *NIST Standard Reference Data Base, Positive Ion Energetics*, Version 2.01, Gaithersburg, MD, **1994**

[9] Reviews: M. Dolg, H. Stoll in *Handbook on the Physics and Chemistry of the Rare Earths*, Vol. 22 (Eds.: K. A. Gschneider Jr., L. Eyring), Elsevier, Amsterdam, **1995**; b) M. Dolg, in *The Encyclopedia of Computational Chemistry*, (Eds.: P. von R. Schleyer, N. L. Allinger, T. Clark, J. Gasteiger, P. A. Kollman, H. F. Schaefer III, P. R. Schreiner), Wiley, Chichester, **1998.**

[10] W. Koch, R. H. Hertwig in *The Encyclopedia of Computational Chemistry*, (Eds.: P. von R. Schleyer, N. L. Allinger, T. Clark, J. Gasteiger, J., P. A. Kollman, H. F. Schaefer III, P. R. Schreiner), Wiley, Chichester, **1998**.

[11] For a compilation of recent theoretical work see: *The Challenge of d and f Electrons*, (Eds.: D. R. Salahub, M. Zerner), American Chemical Society, Washington, DC, **1989**. Also see: A. Hengrasmee, M. M. Probst, *Z. Naturforsch. A* **1990**, *46*, 117; G. Ionova, J. C. Krupa, I. Gerard, R. Guillaumont, *New J. Chem.* **1995**, *19*, 677; T. R. Cundari, S. O. Sommerer, L. A. Strohecker, L. Tippett, *J. Chem. Phys.* **1995**, *103*, 7058; S. Di Bella, G. Lanza, I. L. Fragola, T. J. Marks, *Organometallics* **1996**, *15*, 3985; U. Consentino, G. Moro, D. Pitea, L. Calabi, A. Maiocchi, *J. Mol. Struct. (THEOCHEM)* **1997**, *392*, 75; C. Adamo,

  0947-6539/99/0501-0318 $ 17.50+.50/0 

P. Maldivi, *Chem. Phys. Lett.* **1997**, *268*, 61; W. Küchle, M. Dolg, H. Stoll, *J. Phys. Chem. A* **1997**, *101*, 7128; L. Troxler, A. Dedieu, F. Hutschka, G. Wipff, *J. Mol. Struct. (THEOCHEM)* **1998**, *431*, 151; A. Lesar, G. Muri, M. Hodoscek, *J. Phys. Chem. A* **1998**, *102*, 1170.

[12] M. Dolg, H. Stoll, H. Preuss, *Theochem. (J. Mol. Struct.)* **1992**, *96*, 239.

[13] a) M. Dolg, M., H. Stoll, H. Preuss, *Theor. Chim. Acta.* **1993**, *85*, 441; b) M. Dolg, H. Stoll, H. Preuss, *Chem. Phys.* **1992**, *165*, 21; c) M. Dolg, H. Stoll, H.-J. Fladt, H. Preuss, *J. Chem. Phys.* **1992**, *97*, 1162; d) M. Dolg, H. Stoll, H. Preuss, *Chem. Phys. Lett.* **1992**, *174*, 208; e) M. Dolg, H. Stoll, H. Preuss, *Theochem. (J. Mol. Struct.)* **1991**, *77*, 243; f) M. Dolg, H. Stoll, H. Preuss, H. *Chem. Phys.* **1990**, *148*, 219; g) M. Dolg, H. Stoll, H. Preuss, *J. Chem. Phys.* **1989**, *90*, 1730; h) S. G. Wang, W. H. E. Schwarz, *J. Chem. Phys.* **1995**, *99*, 11687.

[14] C. Heinemann, H. H. Cornehl, D. Schröder, M. Dolg, H. Schwarz, *Inorg. Chem.* **1996**, *35*, 2463.

[15] a) A. D. Becke, *J. Chem. Phys.*, **1993**, *98*, 1372; b) A. D. Becke, *J. Chem. Phys.*, **1993**, *98*, 5648; c) P. J. Stephens, J. F. Devlin, C. F. Chabalowski, M. J. Frisch, *J. Phys. Chem*. **1994**, *98*, 11623.

[16] T. R. Cundari, W. J. Stevens, *J. Chem. Phys.* **1993**, *98*, 5555.

[17] a) T. H. Dunning Jr., *J. Chem. Phys.* **1970,** *53*, 2823; b) T. H. Dunning Jr., P. J. Hay, in *Modern Theoretical Chemistry*, (Ed.: H. F. Schaefer III), Plenum, New York, **1977**.

[18] a) ECPs: M. Dolg, H. Stoll, H. Preuss, *J. Chem. Phys.* **1989**, *90*, 1730; b) basis set for cerium: M. Dolg, unpublished, see http://www.theochem.uni-stuttgart.de; c) basis set for holmium: M. Dolg, personal communication.

[19] J. A. Pople, L. Radom, P. v. R. Schleyer, W. J. Hehre, *Ab Initio Molecular Orbital Theory*, Wiley, Chichester, **1986**, and references therein.

[20] R. J. Gdanitz, R. Ahlrichs, *Chem. Phys. Lett.* **1988**, *143*, 413.

[21] Strictly speaking the wave functions used in the analysis correspond to the Kohn–Sham Slater determinants describing the *non-interacting* reference systems and not the real, interacting species. However, for all practical purposes these wave functions can be analyzed like regular wave functions in conventional ab inito calculations.

[22] a) A. E. Reed, L. A. Curtiss, F. Weinhold, *Chem. Rev.*, **1988**, *88*, 899; b) E. D. Glendening, A. E. Reed, J. E. Carpenter, F. Weinhold, F., NBO version 3.1 as implemented in GAUSSIAN94.

[23] MULLIKEN 2.0: J. E. Rice, H. Horn, B. H. Lengsfield, A. D. McLean, J. T. Carter, E. S. Replogle, L. A. Barnes, S. A. Maluendes, G. C. Lie, M. Gutowski, W. E. Rudge, P. A. Sauer, R. Lindh, K. Andersson, T. S. Chevalier, P.-O. Widmark, D. Bouzida, J. Pacansky, K. Singh, C. J. Gillan, P. Carnevali, W. C. Swope, B. Liu, IBM Almaden Research Center, San Jose CA, **1996**. The M(odified)B3LYP formulation as implemented in the Mulliken program package differs from the B3LYP known from the Gaussian program by use of the Perdew86 local correlation functional instead of the VWN analogue. For a discussion of the effect of different formulations of the B3LYP functional, see: R. H. Hertwig, W. Koch, *Chem. Phys. Lett.*, **1997**, *268*, 345.

[24] MOLPRO is a package of ab initio programs written by H.-J. Werner, and P. J. Knowles, with contributions from J. Almlöf, R. D. Amos, M. J. O. Deegan, S. T. Elbert, C. Hampel, W. Meyer, K. Peterson, R. Pitzer, A. J. Stone, P. R. Taylor, and R. Lindh.

[25] GAUSSIAN94: M. J. Frisch, G. W. Trucks, H. B. Schlegel, P. M. W. Gill, B. G. Johnson, M. A. Robb, J. R. Cheeseman, T. A. Keith, G. A. Petersson, J. A. Montgomery, K. Raghavachari, M. A. Al-Laham, V. G. Zakrzewski, J. V. Ortiz, J. B. Foresman, C. Y. Peng, P. Y. Ayala, W. Chen, M. W. Wong, J. L. Andres, E. S. Replogle, R. Gomperts, R. L. Martin, D. J. Fox, J. S. Binkley, D. J. DeFrees, J. Baker, J. P. Stewart, M. Head-Gordon, C. Gonzales, and J. A. Pople, Gaussian Inc., Pittsburgh PA, **1995**.

[26] a) R. W. F. Bader, *Atoms in Molecules*, Clarendon Press, Oxford, **1994**; b) R. W. F. Bader, *Chem. Rev.* **1991**, *91*, 893.

[27] For similar complexes see, for example, T. K. Dargel, R. H. Hertwig, W. Koch, W., *Mol. Phys.*, in press.

[28] One of the referees pointed out that due the structural similarity betwen TS(3) and Min(4) and the problems with the SCF procedure for the latter, also the B3LYP/BSII energy of TS(3) might be doubtful. We have no explanation why the Kohn–Sham SCF procedure did converge for TS(3) but not for Min(4). However, we obtained a cleanly converged solution for TS(3) and are therefore reluctant to severely question its relative energy.

[29] W. Martin, R. Zalubas, L. Hagan, *Atomic Energy Levels - The Rare Earth Elements*; NSRDS-NBS 60, National Bureau of Standards, Washington DC, **1978**.

Received: July 14, 1998 [F1259]